Modeling the seasonal distribution of planktonic foraminifera during the Last Glacial Maximum

I. Fraile,[1] M. Schulz,[1,2] S. Mulitza,[1,2] U. Merkel,[1,2] M. Prange,[1,2] and A. Paul[1,2]

Received 12 September 2008; revised 23 January 2009; accepted 24 February 2009; published 11 June 2009.

[1] We studied the seasonality of planktonic foraminifera during the Last Glacial Maximum using a foraminifera model coupled to an ecosystem model. The model suggests that the timing of the maximum seasonal production of planktonic foraminifera during the Last Glacial Maximum occurred at a different time of the year from present day. The assumption of "stable" seasonality through time, one of the underlying assumptions in paleoceanographical studies that utilize monospecific samples of planktic foraminifera, is thus mistaken. This finding entails implications for foraminifera-based paleotemperature reconstructions. The change in the timing of maximum foraminiferal production could lead to a bias in estimated paleotemperature if the change in seasonality is not taken into account. The existence of the potential seasonal bias is not a new concept in paleoceanography, but here we assess this bias for the first time from a comprehensive modeling approach. In tropical waters, where temperature seasonality has a relatively small amplitude, the estimated sea surface temperature is close to the annual mean. Thus, variations in foraminiferal seasonality do not cause a significant change in the recorded temperature. By contrast, changes in seasonality have the largest influence on the temperature signal at high latitudes and midlatitudes. Our model prediction suggests that because of the temperature sensitivity of the considered species, during the Last Glacial Maximum, the largest production of foraminifera occurred during a warmer season of the year. In some regions, the maximum foraminiferal production month shifted by up to 6 months. Our findings may help to reconcile low glacial planktonic $\delta^{18}O$ values with proxy evidence for deep-water formation in the Nordic Seas.

Citation: Fraile, I., M. Schulz, S. Mulitza, U. Merkel, M. Prange, and A. Paul (2009), Modeling the seasonal distribution of planktonic foraminifera during the Last Glacial Maximum, *Paleoceanography*, *24*, PA2216, doi:10.1029/2008PA001686.

1. Introduction

[2] Foraminiferal studies provide a fundamental contribution to our understanding of past and future ocean and climate systems. Many paleotemperature reconstructions rely on the analysis of foraminiferal test chemistry or assemblage composition. However, temperature estimates derived using species-specific paleotemperature equations are strongly affected by the seasonality of temperature-sensitive species [*Mulitza et al.*, 1998; *Tedesco et al.*, 2007]. In order to accurately interpret the foraminiferal fossil record preserved within deep-sea sediments, early works focused on modern foraminiferal ecology [e.g., *Bé and Hamilton*, 1967; *Bé and Tolderlund*, 1971; *Hemleben et al.*, 1989]. The development of automated time series sediment traps [*Honjo et al.*, 1980; *Honjo and Doherty*, 1988] has led to a better understanding of the fluxes of modern planktonic foraminifera, revealing that they have large seasonal variations in abundance tied closely to surface water hydrography [*Bé*, 1960; *Bé and Tolderlund*, 1971; *Deuser et al.*, 1981; *Thunell and Honjo*, 1987; *Sautter and Thunell*, 1991]. Different foraminifera species have distinct seasonal patterns, the imprint of which is preserved in the sedimentary record [*King and Howard*, 2005; *Schiebel and Hemleben*, 2005]. Thus, the temperature signature found in the sedimentary record lies between the annual mean water temperature and the preferred temperature of a particular species [*Mix*, 1987].

[3] The seasonal distribution of some foraminiferal species can change through time as climate changes, leading to a bias in estimated paleotemperature. This variation needs to be quantified in order to better constrain the interpretation of foraminifera-based sea surface temperature (SST) reconstructions. To study the seasonal variations of planktonic foraminifera species at glacial-interglacial timescales, we use a foraminiferal numerical model [*Fraile et al.*, 2008]. This planktonic foraminiferal model predicts monthly concentrations of five species within the global mixed layer. In order to test the response of planktonic foraminifera to climate changes, the model has been run for modern conditions and for the Last Glacial Maximum (LGM). This study shows model predictions for spatial and temporal distributions of five most frequently used foraminiferal species, and discusses the implications for paleotemperature reconstructions.

2. Methods

2.1. Foraminifera Model and Experimental Setup

[4] The model predicts monthly concentrations of the following planktonic foraminifera species: *N. pachyderma*

[1]Faculty of Geosciences, University of Bremen, Bremen, Germany.
[2]MARUM, University of Bremen, Bremen, Germany.

0883-8305/09/2008PA001686$12.00

(sinistral and dextral varieties), *G. bulloides*, *G. ruber* (white variety) and *G. sacculifer*. These species are mostly found in the euphotic zone, and reflect the sea surface environment [*Bé*, 1982]. The model is implemented into an ecosystem model [*Moore et al.*, 2002], from which it takes information on food availability for the foraminifera. Species specific food preferences and temperature tolerance ranges are derived from sediment trap studies and laboratory cultures [*Hemleben et al.*, 1989; *Bijma et al.*, 1990; *Watkins et al.*, 1996; *Watkins and Mix*, 1998; *Arnold and Parker*, 1999; *Žarić et al.*, 2005]. Accordingly, the change in foraminiferal concentration depends on the growth and mortality rates of the population, as follows in this equation:

$$\frac{dF}{dt} = (GGE \cdot TG) - ML \quad (1)$$

[5] Here, F is the foraminifera carbon concentration, and GGE (gross growth efficiency) is the portion of grazed matter that is incorporated into foraminifera biomass, and TG and ML represent total grazing and mass loss, respectively. The total grazing is calculated on the basis of food availability and temperature sensitivity of the species. On the basis of the compilation planktonic foraminiferal fluxes from sediment trap observations across the World Ocean [*Žarić et al.*, 2005], the relationship with temperature has been approximated to a Gaussian distribution. The assumption of a Gaussian pattern, with a central peak and symmetrical tails, seems to be supported by these sediment trap data, although a non symmetrical response to temperature have also been observed by other authors during laboratory cultures [*Lombard et al.*, 2009]. The mass loss (mortality) equation comprises three terms representing losses due to natural death rate (respiration loss), predation by higher trophic levels and competition.

[6] Initially, the model was run for 2 years as spin-up, to allow an equilibrium state to be reached [*Moore et al.*, 2002]. The monthly data from a third year were then saved. Each grid point was run independently with a longitudinal resolution of 3.6°, and a varying latitudinal resolution between 1° and 2° (higher resolution near the equator). The ecosystem foraminifera model was forced with physical and chemical boundary conditions. In the model standard setup, the forcing includes SST (World Ocean Atlas 1998 [*Conkright et al.*, 1998]), surface shortwave radiation [*Bishop and Rossow*, 1991; *Rossow and Schiffer*, 1991], climatological mixed layer depths [*Monterey and Levitus*, 1997], vertical velocity at the base of mixed layer [*Gent et al.*, 1998], turbulent exchange rate at the base of the mixed layer (constant value of 0.15 m/day [*Moore et al.*, 2002]), sea ice coverage [*Cavalieri et al.*, 1990] and atmospheric iron flux [*Mahowald et al.*, 1999]. The foraminifera model and its behavior in a global surface mixed layer is described in detail by *Fraile et al.* [2008].

[7] To compare the foraminiferal response to glacial-interglacial periods, we used the global coupled Community Climate System Model version 3 (CCSM3) [*Collins et al.*, 2006] to force the foraminifera model. We carried out experiments for two different environmental conditions: in the standard run the model was forced with present-day conditions (PD), using the same forcing as described by *Fraile et al.* [2008], and in the second run with Last Glacial Maximum conditions (LGM).

[8] We also performed sensitivity experiments to evaluate the influence of nutrients on foraminiferal populations. We carried out an experiment increasing the nutrient concentrations below the mixed layer by 3.2% for the LGM, equivalent to the increase resulting from a 120 m eustatic sea level lowering [*Fairbanks*, 1989]. Finally, we performed another experiment using the nutrient (nitrate and phosphate) distributions below the mixed layer as simulated by the University of Victoria Earth System Climate Model (UVic ESCM) for the LGM [*Weaver et al.*, 2001]. For this experiment, we calculated the difference in nutrient concentration between preindustrial and LGM conditions within the UVic, and we applied this anomaly to our standard LGM run.

2.2. CCSM3 Climate Model Simulations

[9] The National Center for Atmospheric Research (NCAR) CCSM3 is a state-of-the-art coupled climate model. The global model is composed of four separate components representing atmosphere, ocean, land, and sea ice [*Collins et al.*, 2006]. Here, we use the low-resolution version of CCSM3 which is described in detail by *Yeager et al.* [2006]. In this version, the resolution of the atmospheric component is given by T31 (3.75° by 3.75° transform grid) spectral truncation with 26 layers, while the ocean has a mean resolution of 3.6° by 1.6° (like the sea ice model) with 25 levels. The latitudinal resolution of the oceanic model grid is variable, with finer resolution near the equator (≈0.9°).

[10] We have performed two coupled climate simulations (preindustrial and LGM), the results of which were used to force the ecosystem and foraminifera model. The preindustrial simulation uses forcing appropriate for conditions before industrialization and follows the protocol established by the Paleoclimate Modeling Intercomparison Project, Phase 2 (PMIP-2; http://www-lsce.cea.fr/pmip2/) [*Braconnot et al.*, 2007]. This forcing represents the average conditions of the late Holocene before the significant impact of humans, rather than a specific date, and it includes concentrations of greenhouse gases, changes in the spatial distributions of ozone, sulfate (only direct effect), and carbonaceous aerosols [*Otto-Bliesner et al.*, 2006a, 2006b]. In addition to these forcing factors, changes in orbital parameters, ice sheets and a reduced global sea level are taken into account for the LGM (21,000 years before present) simulation following the PMIP-2 protocol. For continental ice sheet extent and topography, the LGM ICE-5G reconstruction [*Peltier*, 2004] is used. The coastline is also taken from ICE-5G and corresponds to a sea level lowering of ≈120 m such that new land is exposed.

[11] Both climate simulations were integrated for more than 600 years so that the surface climatologies reached a statistical equilibrium and could be used for ecosystem model forcing. The mean of the last 100 simulation years of the following parameters was used to force the ecosystem and foraminifera models: SST, mixed layer depth, ice fraction, shortwave radiation and vertical velocity at the base of mixed layer. The glacial cooling of the tropical surface ocean is up to 2°C. Stronger cooling (>5°C) takes

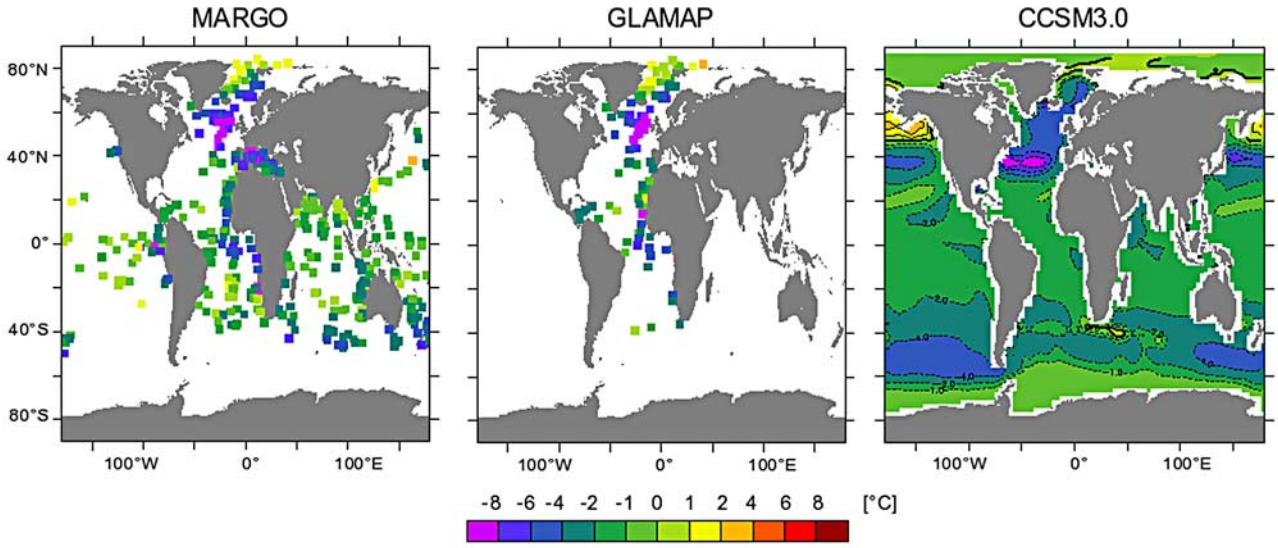

Figure 1. (left and middle) Average annual SST anomaly between the Last Glacial Maximum and modern conditions (LGM-WOA) estimated from planktonic foraminifera (MARGO data set [*Weinelt et al.*, 2004] and GLAMAP 2000 compilation [*Pflaumann et al.*, 2003]) and (right) SST anomaly (LGM-PI) simulated by CCSM3.0.

place at high latitudes. The largest temperature drop can be found in the North Atlantic, where glacial temperatures are up to 10°C colder than preindustrial values (Figure 1). The North Atlantic temperature drop can partly be explained by a reduction of the meridional overturning circulation. In the LGM simulation, the overturning weakens by nearly one third from 14 sverdrups (Sv) in the preindustrial run to about 10 Sv (not shown). The core depth of southward flowing North Atlantic Deep Water (i.e., the Deep Western Boundary Current) reduces from ~2500 m in the preindustrial simulation to ~1500 m in the glacial run. The peak northward heat transport in the North Atlantic ocean decreases by about 20% in the LGM. Further details of the model experiment will be presented elsewhere (U. Merkel et al., manuscript in preparation, 2009).

[12] We calculated the anomaly of the forcing variables (SST, mixed layer depth, ice fraction, shortwave radiation and vertical velocity at the base of the mixed layer) simulated by CCSM3 between LGM and preindustrial conditions, and we added this anomaly to the standard forcing data as an LGM forcing for the foraminiferal model. We used this approach in order to reduce deviations induced by the climate model errors. For example, in the North Atlantic, the SSTs simulated by CCSM3 for present day are up to 7°C too low compared to World Ocean Atlas data [*Prange*, 2008]. Glacial SST anomalies correspond well with reconstructions (Figure 1). In order to avoid potential inconsistencies between sea ice fraction and SST, we set ice fraction to zero for temperatures above −1.5°C.

2.3. UVic Earth System Climate Model Simulations

[13] For an experiment on foraminiferal sensitivity to changes in the nutrient distributions, we used the output from the UVic ESCM (version 2.8). Compared to CCSM3, the atmospheric component is simplified and consists of a vertically integrated two-dimensional energy-moisture balance model [*Weaver et al.*, 2001]. In addition to the atmosphere, ocean and sea ice components, it contains a land surface scheme [*Cox*, 2001], a dynamic global vegetation model [*Cox et al.*, 1999; *Meissner et al.*, 2003] and a marine biogeochemical component [*Schmittner et al.*, 2005].

[14] The horizontal resolution of the model is constant at 3.6° in the longitudinal and 1.8° in the latitudinal direction and thus comparable to CCSM3. In the ocean component, there are 19 levels in the vertical direction with a thickness ranging from 50 m near the surface to 590 m near the bottom.

[15] In both (preindustrial and LGM) simulations carried out with the UVic ESCM, the monthly wind stress to force the ocean and monthly winds for the advection of heat and moisture in the atmosphere are prescribed from the NCEP reanalysis climatology [*Kalnay et al.*, 1996]. The model is driven by the seasonal variation of insolation, appropriate to either preindustrial or LGM conditions. As in CCSM3, the ICE-5G reconstruction [*Peltier*, 2004] is used to prescribe the continental ice sheet extent and topography for the LGM. Because of the computational efficiency of the UVic ESCM, the simulations could be integrated for more than 10,000 years and reached quasi-equilibrium conditions even in the deep ocean, with a cooling of the sea surface between ≈2°C in the tropics and ≈10°C in the high-latitude North Atlantic. For further details, see A. Paul et al. (manuscript in preparation, 2009) and *Weaver et al.* [2001].

2.4. Sedimentary Faunal Assemblages

[16] To compare our model prediction of planktonic foraminiferal distribution during the LGM with sediment data, we used planktonic foraminifera census data from the MARGO [*Barrows and Juggins*, 2004; *Kucera et al.*, 2004a, 2004b; *Niebler*, 2004; *Kucera et al.*, 2005a, 2005b; *Waelbroeck et al.*, 2009] and GLAMAP (supplementary

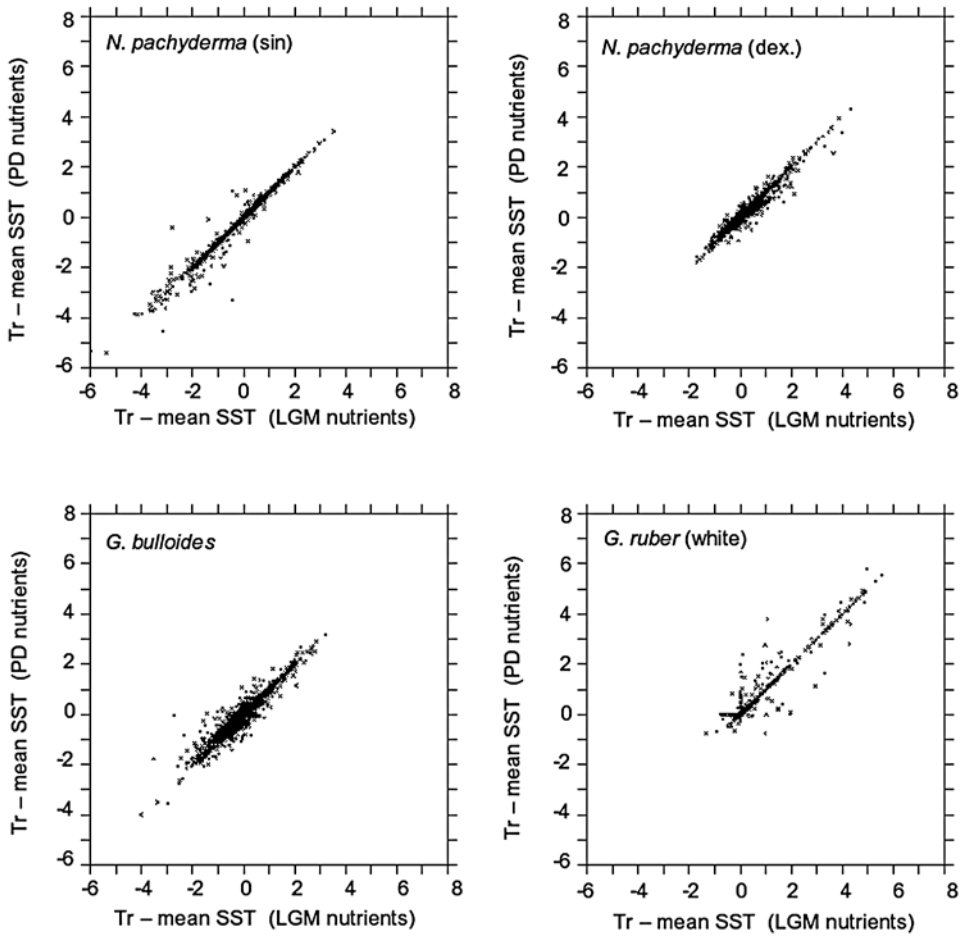

Figure 2. Comparison of the recorded signal during the LGM in two model experiments. The departure from the annual mean SST (flux-weighted annual mean signal recorded by the species, Tr, minus annual mean SST, in °C) is used to evaluate the similarity of the two experiments. Model-based reconstruction using NO_3 and PO_4 redistribution below mixed layer simulated by the UVic Earth System Climate Model versus model-based reconstruction using present-day nutrient distribution below mixed layer.

data set, http://doi.pangaea.de/10.1594/PANGAEA.692144 [see *Pflaumann et al.*, 2003]) data sets. For present day we used core top data from the Brown University Foraminiferal Database [*Prell et al.*, 1999], extended with the data set by *Pflaumann et al.* [1996] for the Atlantic, and with samples from the eastern Indian Ocean [*Martinez et al.*, 1998]. For comparison, the relative abundances were recalculated using only the five foraminifera species under consideration. The number of individuals was transformed into biomass (mgC/m^3) to take into account the size differences of each species. The transformation was made following the same procedure as in the work by *Fraile et al.* [2008].

2.5. Flux-Weighted Temperature Signal

[17] Seasonal variations in the abundance of the species have been studied to evaluate their implications for proxy records. The isotopic (or trace element) composition of a foraminiferal population in the sediment is the flux-weighted mean of all isotope values. Thus, theoretically, the temperature sensed by the mean population of a species (T_r) is the flux-weighted mean of all temperatures at the site. We calculated the theoretical mean SST recorded in each of the respective species (T_r):

$$T_r = \frac{\sum_{m=1}^{12} (C_m \cdot T_m)}{\sum_{m=1}^{12} C_m} \quad (2)$$

where C_m is monthly species concentration and T_m denotes SST. At each site, T_r ranges between the mean water temperature and mean preferred temperature by the species [*Mix*, 1987]. Theoretically, T_r corresponds to the signal found in the sedimentary record.

3. Results

3.1. Relative Abundances of the Species During the LGM

[18] The sensitivity experiment with increased nutrient concentrations below the mixed layer by 3.2% does not

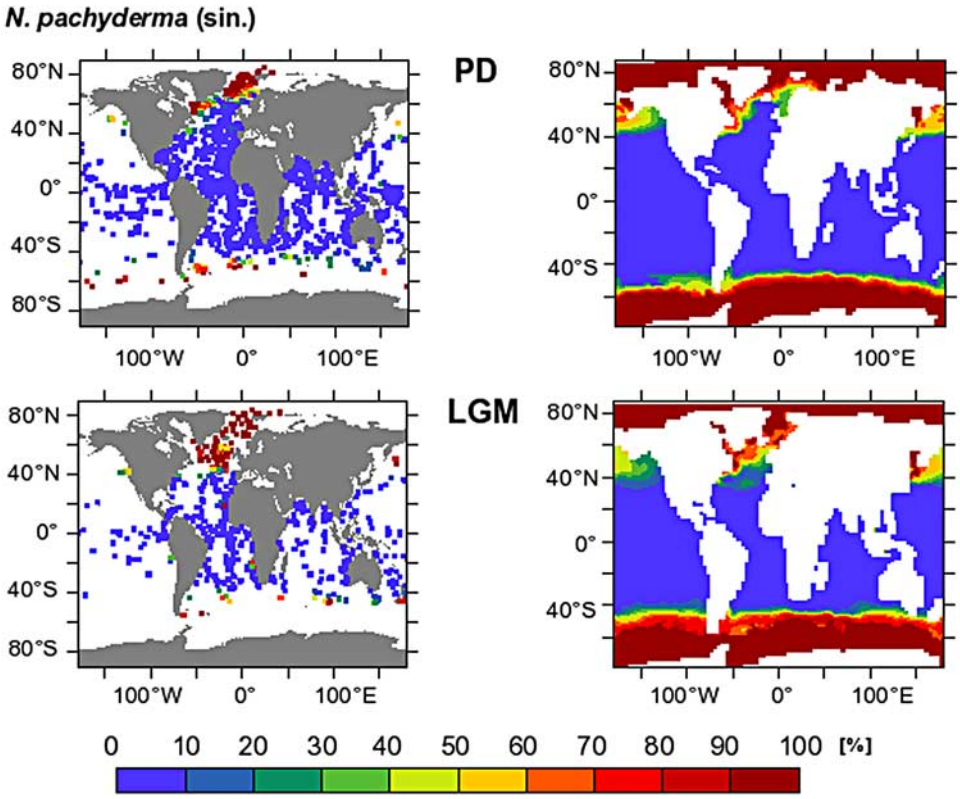

Figure 3. Relative abundance of *N. pachyderma* (sinistral) (top) for modern conditions and (bottom) during the LGM in the (left) sedimentary record and (right) model prediction. Relative abundances consider only the five species included in the model. Modern sedimentary faunal assemblage data are from *Pflaumann et al.* [1996], *Prell et al.* [1999], and *Martinez et al.* [1998], and LGM data are from MARGO and GLAMAP data sets [*Barrows and Juggins*, 2004; *Kucera et al.*, 2004a, 2004b; *Niebler*, 2004; *Kucera et al.*, 2005b; *Pflaumann et al.*, 2003].

show a significant effect in foraminiferal concentration (total biomass variation $\leq$1% for all species). Using the nutrient redistribution below the mixed layer simulated with UVic ESCM lead to more pronounced changes in the abundance of foraminifera is more pronounced (total biomass variation between 3 and 6%). When applying these variations to temperature reconstructions, the influence becomes even smaller. Figure 2 illustrates the correlation between the experiments using standard nutrient distribution below mixed layer and the redistribution simulated by the UVic model. For the four species the differences between both experiments are very small.

[19] Therefore, to compare with sediment samples, nutrient concentrations below the mixed layer were kept the same as in the work by *Moore et al.* [2002] for both modern and LGM runs. Figures 3, 4, 5, 6, and 7 illustrate annual mean relative abundances predicted by the model as compared to those measured in sediments for the five different species.

[20] The global abundance pattern of *N. pachyderma* (sinistral) in sediments, as well as in the model prediction, yield highest relative abundances (up to 100%) in polar waters (Figure 3, top). In comparison with present-day conditions, the area of dominance of *N. pachyderma* (sinistral) during the glacial period is wider (Figure 3, bottom). In particular, its distribution in the North Atlantic spreads southward to lower latitudes. The lack of foraminiferal census data in the Southern Ocean hampers model evaluation in this region. Both model and sedimentary data indicate that *N. pachyderma* (dextral) and *G. bulloides* occurred in significant numbers in the major upwelling areas (Figures 4 and 5, respectively, top). Along 40°S, the model predicts a dominance of *G. bulloides* over the other four species, which is also reflected by the sediments south of Australia. The distribution of *N. pachyderma* (dextral) and *G. bulloides* during the LGM also extends toward lower latitudes compared to present day (Figures 4 and 5, respectively, bottom). However, the model overestimates their relative abundance in tropical waters, between 20°N and 20°S, where, away from upwelling regions, the relative abundances in the sediments are $\leq$10% (Figures 4 and 5, bottom left). By contrast, the model predicts relative abundances between 20 and 40% during the LGM (Figures 4 and 5, bottom right). As a consequence, the predicted relative abundance of *G. ruber* (white) at these latitudes is too low (Figure 6, bottom right). *G. sacculifer* is limited to tropical waters, but its abundance is also underestimated, more

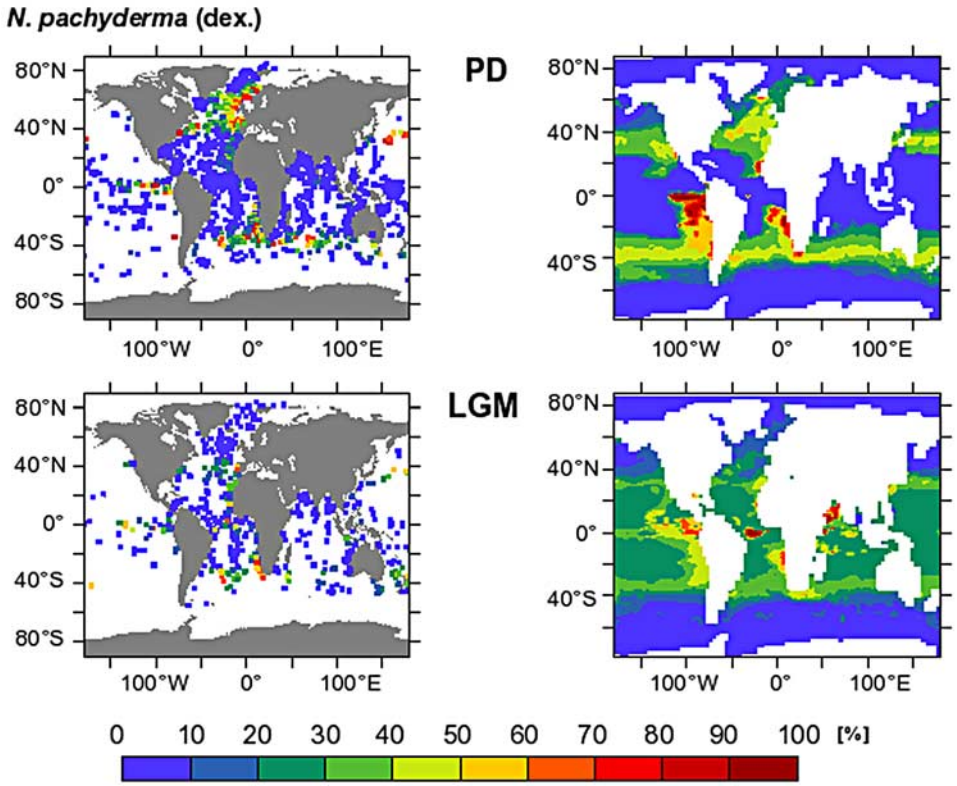

Figure 4. Relative abundance of *N. pachyderma* (dextral) (top) for modern and (bottom) during the LGM in the (left) sedimentary record and (right) model prediction. Symbols and layout of the graphs are the same as in Figure 3.

pronounced in the Atlantic Ocean than in the Pacific and Indian Oceans (Figure 7, bottom).

3.2. Foraminiferal Seasonality During the LGM

[21] The signal recorded by *N. pachyderma* (sinistral) and *G. bulloides* during the LGM is found to be biased toward summer conditions at high latitudes (polar/subpolar waters for *N. pachyderma* (sinistral), and between 40° and 60°N/S for *G. bulloides*), and toward winter below 40° latitude (Figures 8a and 8c). In contrast, for *N. pachyderma* (dextral) and *G. ruber*, the seasonal imprint on T_r becomes only discernible at the edge of their distributions (poleward of 40°N/S for *N. pachyderma* (dextral) and 35°N/S for *G. ruber*), where the signal is biased toward summer conditions (Figures 8b and 8d). At lower latitudes the recorded temperature signal is close to annual mean SST. Our model predicts that *G. sacculifer* limited to tropical waters, where temperature in open ocean has little variability through the year. In consequence, the temperature signal recorded by *G. sacculifer* in tropical waters reflects mostly annual mean conditions [*Fraile et al.*, 2009]. Any variability in the seasonal cycle of *G. sacculifer* would thus have little influence on the proxy signal. Therefore, it is not shown in Figures 9, 10, 11, and 12.

[22] Figures 9–12 illustrate the maximum production month of each species predicted by the model for PD and LGM. It has to be noted that in regions where the annual distribution pattern has low variability (e.g., in the tropics or at regions where the annual foraminiferal cycle is typically bimodal), the maximum production month does not always have a significant imprint on the recorded temperature. In regions with a wide seasonal maximum or with a double peak only the absolute maximum is taken into account, resulting in a noisy pattern. In order to reduce this noise, the original data have been smoothed using a boxcar filter along both axes by three grid points. During the LGM the maximum production month coincides more often with summer months compared to the modern situation. For example, according to the model, *N. pachyderma* (sinistral) presently occurs during summer months poleward of 60° latitude, and during spring between 40° and 60° latitude (Figure 9, left). During the LGM, the maximum production occurred during summer above 30° latitude, more evident in the southern hemisphere (Figure 9, middle). The right-hand plots of Figures 9–12 show the shift of maximum production month from LGM to present conditions. Thus, positive values indicate that during the LGM maximum production occurred later in the year.

[23] The model simulation suggests that the maximum production month could have shifted considerably between PD and LGM conditions, producing a large seasonal bias (Figures 9–12, right). The results show a very variable response for each species: Maximum seasonal bias for *N. pachyderma* (sinistral) and *G. bulloides* occurs in the subantarctic front, around 60°S and 40°S respectively

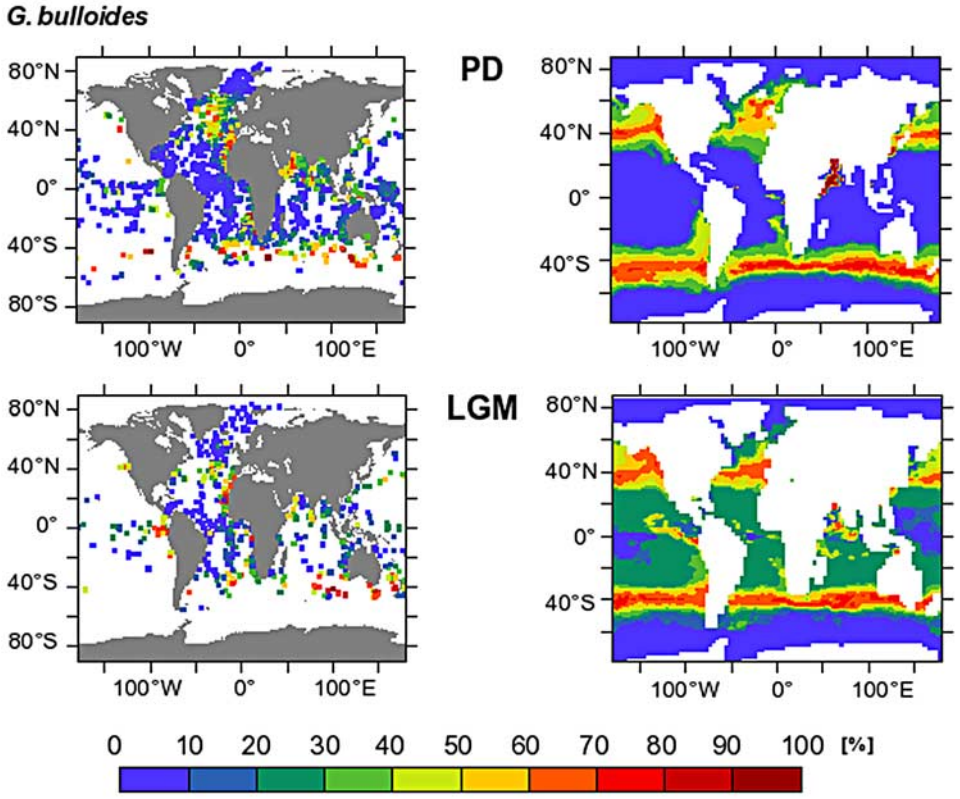

Figure 5. Relative abundance of *G. bulloides* (top) for modern and (bottom) during the LGM in the (left) sedimentary record and (right) model prediction. Symbols and layout of the graphs are the same as in Figure 3.

(Figures 9 and 11, right). In case of *N. pachyderma* (dextral) the largest change in seasonality takes place between 30° and 40°N in the North Atlantic Ocean, where maximum production is shifted by up to 6 months (Figure 10, right). *G. ruber* (white) experiences a maximum shift of seasonality in tropical waters (Figure 12, right). Nevertheless, variations in foraminiferal seasonality in tropical waters do not affect the isotopic signal considerably, as temperature seasonality is small.

4. Discussion

4.1. Comparison Between Model Output and Sediment Samples

[24] The distribution patterns of all species during the LGM are shifted to lower latitudes in response to the glacial cooling. According to our model prediction, during the LGM, *N. pachyderma* (sinistral) extended its distribution to lower latitudes (Figure 3), in response to favorable cold temperatures found between 40° and 50° latitude. During the LGM, the spatial distribution was wider compared to that for modern conditions, especially in the southern hemisphere. Core data and the model prediction compare favorably, although the lack of glacial sediment samples in the subantarctic region hampers the evaluation in this region.

[25] Maximum cooling occurred around 40°–50°S and between 30° and 50°N in the North Atlantic (more than 4°C cooling (Figure 1)). This cooling causes the distribution of foraminifera inhabiting these regions (mainly *G. bulloides* and *N. pachyderma* (dextral)) to be shifted toward warmer waters (Figures 4 and 5). In tropical waters, model predicted relative abundance of these species during the LGM is overestimated in comparison with sediment samples. Core data suggest that during the LGM the population of *N. pachyderma* (dextral) was diminished in response to unfavorable cold conditions (Figure 4, bottom left). Instead, according to our predictions, the population was shifted to warmer regions rather than being reduced (Figure 4, bottom right). In the case of *G. bulloides* the sedimentary record in the North Atlantic Ocean shows a clear shift in its dominance area: at present day it occurs mainly between 40° and 50°N, whereas during the LGM, north of 40°N its relative abundance was very low (<10%) (Figure 5, left). This shift in the dominance area from low to higher latitudes fits well with the model prediction. The overestimation of *G. bulloides* and *N. pachyderma* (dextral) in tropical waters brings as consequence the underestimation of the relative abundance of *G. ruber* (white) (Figure 6).

[26] Increasing nutrient concentration below mixed layer by 3.2%, equivalent to the increase resulting from a 120 m eustatic sea level lowering [*Fairbanks*, 1989] has a relatively small effect in the biomass of phytoplankton and zooplankton (5–10% and ≤1% respectively). However, the redistribution of NO_3 and PO_4 simulated by UVic seems to

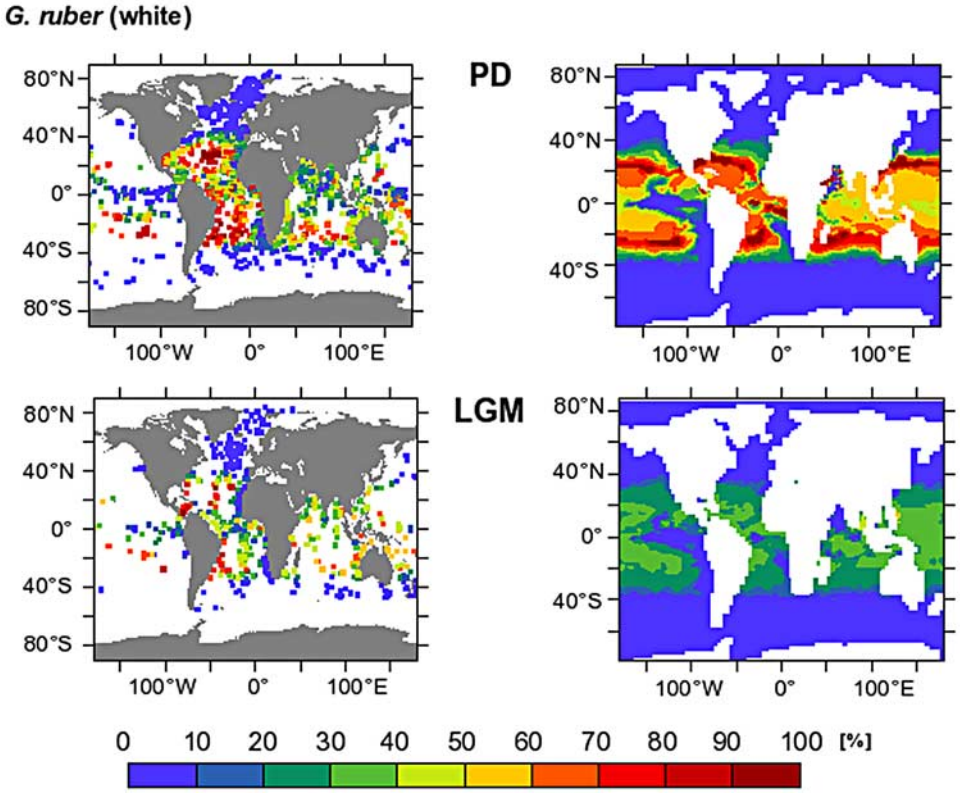

Figure 6. Relative abundance of *G. ruber* (white) (top) for modern and (bottom) during the LGM in the (left) sedimentary record and (right) model prediction. Symbols and layout of the graphs are the same as in Figure 3.

have a greater influence in the productivity (total biomass variation of 10–50% for phytoplankton and around 6% for zooplankton). Total biomass variation of the foraminifera varies at the same scale as zooplankton. However, these variations in the biomass do not seem to be sufficient to alter the biomass-weighted annual mean temperature signal recorded by the species (Figure 2).

4.2. Influence of Seasonality on Temperature Reconstructions

[27] Climate change can induce variations in the seasonality of foraminifera. Changes in the timing of maximum foraminiferal production may influence the proxy signal and lead to a bias in estimated paleotemperature. The concept of the seasonal bias may not be new, but here it is derived for the first time from model simulations. Figure 13 illustrates some examples where, according to our model prediction, a shift in seasonality from LGM to present-day conditions was noted. The maximum production peak is sometimes clearly shifted (Figures 13a, 13c, and 13d), whereas in some other cases the double peak is transformed into a single maximum (Figure 13b).

[28] The largest differences between present-day and LGM conditions are found in the Southern Ocean and in the North Atlantic (Figures 9–11). In particular, in the western North Atlantic glacial cooling is very pronounced, and as a consequence the maximum production month of *N. pachyderma* (sinistral) and *G. bulloides* occurs later in the year, coinciding with the warmest season.

[29] In some cases maximum production shifted by up to 6 months (Figures 9–12). This implies a considerable variation in recorded temperature. For example, our experiment with present day conditions suggests that, around 40°N in the North Atlantic, the isotopic signature in *G. bulloides* is biased toward winter temperatures [*Fraile et al.*, 2009], whereas during the LGM, it was biased toward summer conditions (Figure 8c). As a consequence, using *G. bulloides* to reconstruct glacial SST in this region would underestimate the entire temperature variation by up to 2°C in the eastern North Atlantic and up to 6°C in the western region. Similarly, the change in seasonality of *N. pachyderma* (sinistral) in the subantarctic front, between 40° and 60°S, influences the interpretation of the temperature signal: During the LGM, the distribution of *N. pachyderma* (sinistral) spreads equatorward and maximum production occurred later in the year (Figure 9, right); thus, the mean population would record little change in the temperature signal.

[30] Another interesting feature of the model output is the difference of the recorded signal by *N. pachyderma* (sinistral) in the western and eastern North Atlantic. According to the LGM simulation, in the western and eastern regions of the North Atlantic, around 40°–50°N *N. pachyderma* (sinistral) records a temperature signal

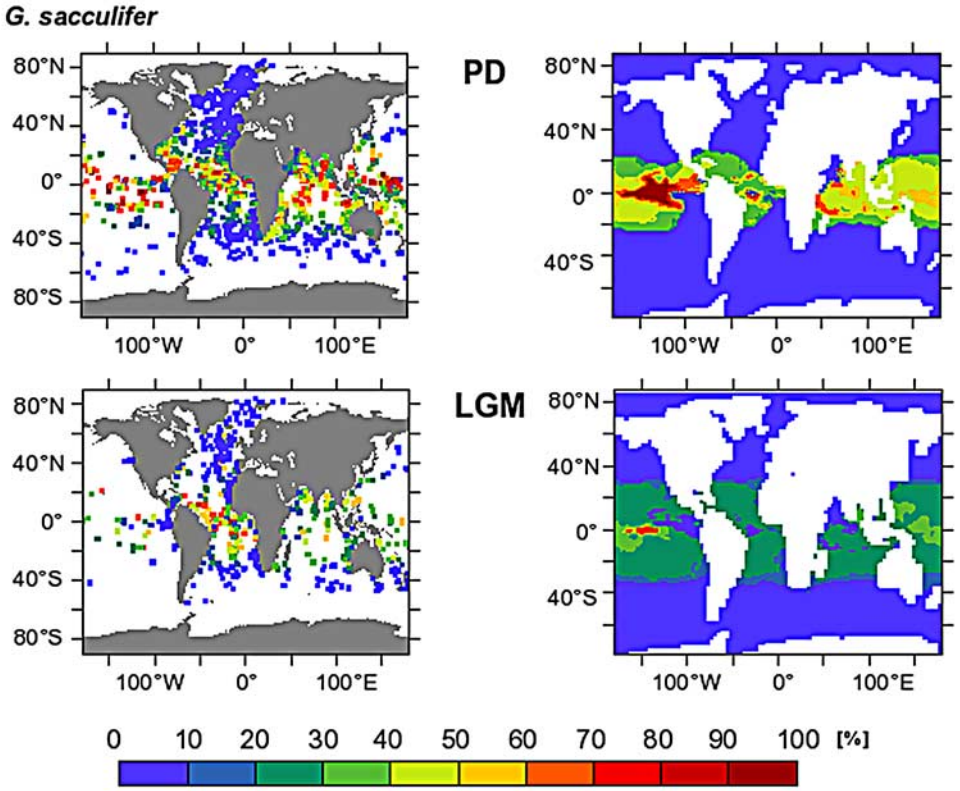

Figure 7. Relative abundance of *G. sacculifer* (top) for modern and (bottom) during the LGM in the (left) sedimentary record and (right) model prediction. Symbols and layout of the graphs are the same as in Figure 3.

above the annual mean; that is, it lives mostly during summer, whereas in the central North Atlantic the recorded signal is biased toward winter (Figure 8a). The GLAMAP reconstruction at North Atlantic subpolar waters based on planktonic foraminifera, one of the major departures from the CLIMAP (1981) pattern, was characterized by an anticyclonic gyre of warm water transported from the western Atlantic margin (summer SSTs of 5°–7°C), and a cold current in the eastern North Atlantic, along the ice-covered British Isles penetrating into the center of the gyre (summer SSTs of 3°–4°C) [*Pflaumann et al.*, 2003]. This pattern with a cold gyre center and a warm surrounding current is difficult to explain physically, and the authors also discuss the possibility of an artifact resulting from lateral advection of polar fauna. According to our model prediction it could just be due to the fact that in the central North Atlantic the temperature signal corresponds to a winter signal, whereas in the western North Atlantic foraminifera record a summer signal.

[31] Another example can be illustrated when applying the model results to the salinity reconstruction of the North Atlantic. *Duplessy et al.* [1991] used the isotopic composition of *N. pachyderma* (sinistral) and *G. bulloides* to reconstruct surface salinity during the LGM in the North Atlantic Ocean, assuming that the isotopic composition of foraminiferal shells is linearly related to summer SST. They reconstructed the seawater δ^{18}O anomaly at the LGM, and explained the positive anomaly as a high-salinity water mass. From these isotopic data, the authors reconstructed a tongue of highly saline surface water which penetrated to the central Atlantic up to 53°N, south of Iceland (Figure 14). They also found a negative anomaly in δ^{18}O of seawater (interpreted as low salinity) in the Norwegian-Greenland seas, northeast of Iceland, and concluded that this was due to both the disappearance of the North Atlantic drift and the input of freshwater resulting from local precipitation and ice melting. On the basis of this paleosalinity distribution, *Labeyrie et al.* [1992] and *Sarnthein et al.* [1994] suggested that the major site of glacial North Atlantic deepwater formation was shifted to the central North Atlantic. However, our model prediction for *N. pachyderma* (sinistral), which accounts for more than 98% of the total foraminifera assemblage [*Pflaumann et al.*, 1996], suggests that the differential seasonality in the Norwegian-Greenland seas and in the central Atlantic, south of Iceland, may have played a role in the isotopic signature. According to our model, north of Iceland, maximum production of *N. pachyderma* (sinistral) occurred from July to August (Figure 15). In contrast, south of Iceland, between 30° and 60°N, where Duplessy and coauthors found a low δ^{18}O anomaly (interpreted as high salinity), occurred from May to July. The difference of 1 or 2 months in the seasonal production translates into a change of $\geq$1°C in the recorded temperature signal, which corresponds to a reduction of the δ^{18}O

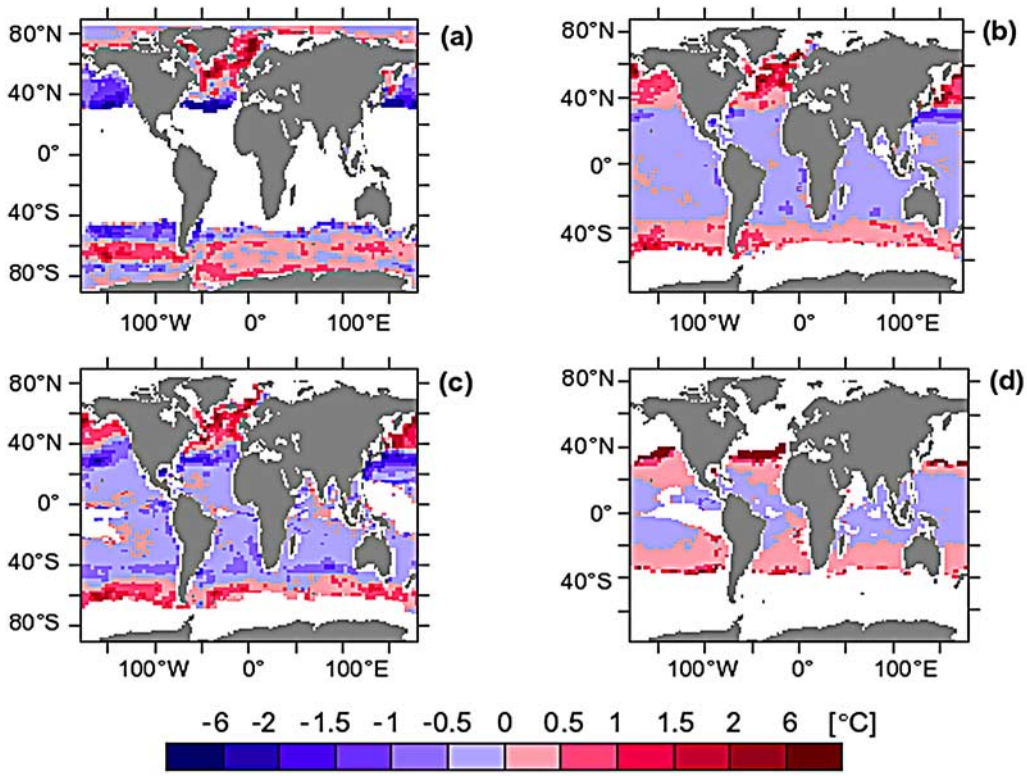

Figure 8. Temperature signal recorded by the species (T_r) minus annual mean SST during LGM for (a) *N. pachyderma* (sinistral), (b) *N. pachyderma* (dextral), (c) *G. bulloides*, and (d) *G. ruber* (white). Values around zero: T_r corresponds to annual mean SST. Negative and positive values: T_r is dominated by winter and summer conditions, respectively.

anomaly of about 0.3. The negative anomalies in $\delta^{18}O$ found by *Duplessy et al.* [1991] in the Norwegian Sea (northeast of Iceland) could therefore be due to the fact that in the Norwegian-Greenland seas *N. pachyderma* (sinistral) calcified later in the year compared to the central Atlantic, and therefore recorded an isotopic signal corresponding to warmer conditions. Hence, the negative anomaly would be a consequence of temperature rather than of low salinity. Similar findings have also been presented by other scientist. For example, on the basis of oxygen isotope records,

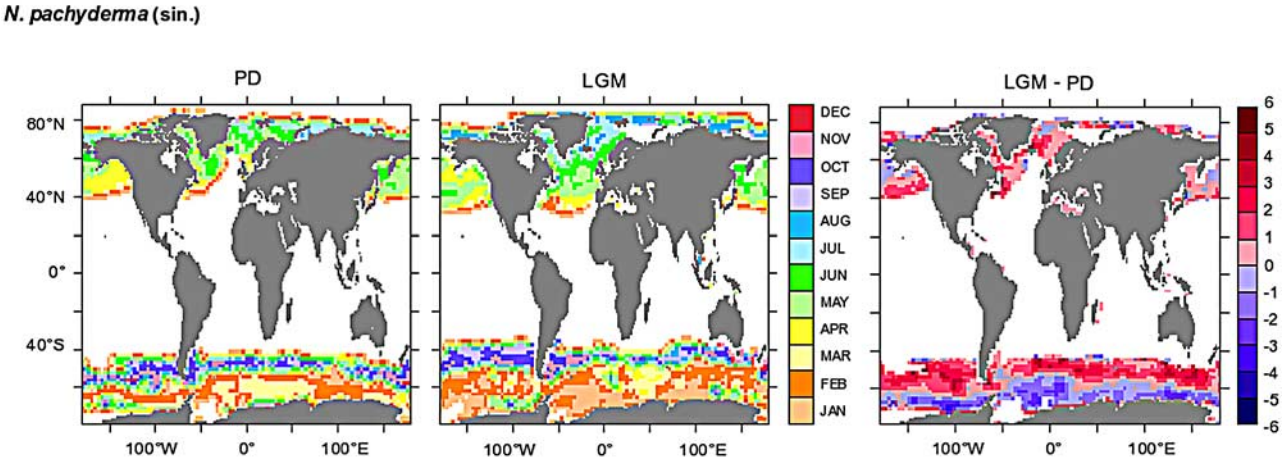

Figure 9. Maximum production month of *N. pachyderma* (sinistral) at present day (PD), Last Glacial Maximum (LGM), and the difference between both (in months). Positive values indicate that during the LGM the maximum production was later in the year.

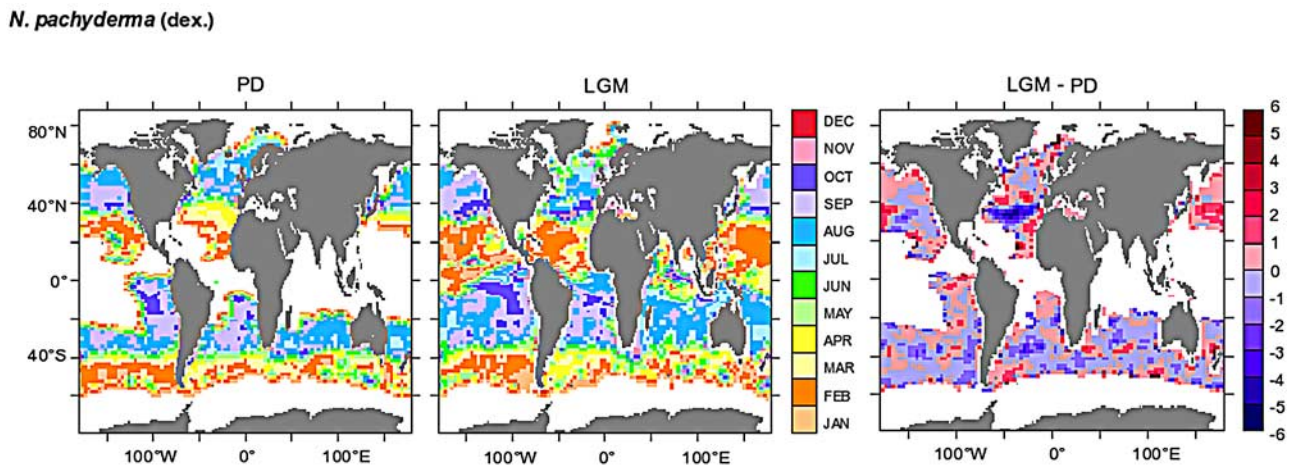

Figure 10. Maximum production month of *N. pachyderma* (dextral) at PD, LGM, and the difference between both (in months). Positive values indicate that during the LGM the maximum production was later in the year.

Sarnthein et al. [1995] suggested that the LGM is characterized as a period of climatic stability and minimum meltwater flux. With a reduced input of freshwater it would indeed be difficult to create a low-salinity surface water mass in the Norwegian-Greenland seas as suggested by *Duplessy et al.* [1991]. If the difference in the isotopic signature north and south of Iceland is due to the differential seasonality of foraminifera, as indicated our model, the surface water in the Norwegian Sea would, in this case, be dense enough for deepwater formation, as suggested by later studies [*Weinelt et al.*, 1996; *Schäfer-Neth and Paul*, 2001].

[32] For tropical species, shifts in seasonality do not seem to have major implications for paleoceanographic reconstructions. For example, the month of maximum production of *G. ruber* (white) and *G. sacculifer* shifted considerably between PD and LGM conditions between 20°S and 20°N. However,the flux-weighted temperature signal in tropical waters was found to be in agreement with the annual mean SST, suggesting the lack of a seasonal bias in foraminifera-based proxy records (Figure 8). In subtropical waters, at the edge of its thermal distribution *G. ruber* (white) records summer conditions during the LGM, similar to those observed under modern conditions.

5. Conclusions

[33] Our foraminifera model simulation suggests that the seasonality of foraminifera has changed from the LGM to the present day. This variation in the annual distribution pattern varies with the species and the oceanic region. In general, the changes in seasonality were greatest at the edge of the distribution of each species, where temperatures are at the lower limit of their tolerance range. During the LGM,

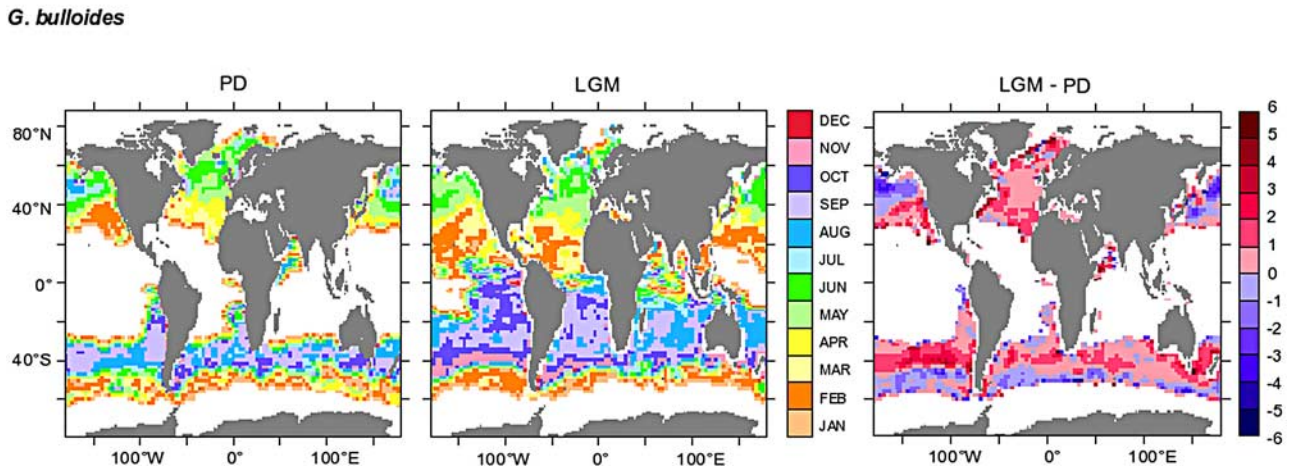

Figure 11. Maximum production month of *G. bulloides* at PD, LGM, and the difference between both (in months). Positive values indicate that during the LGM the maximum production was later in the year.

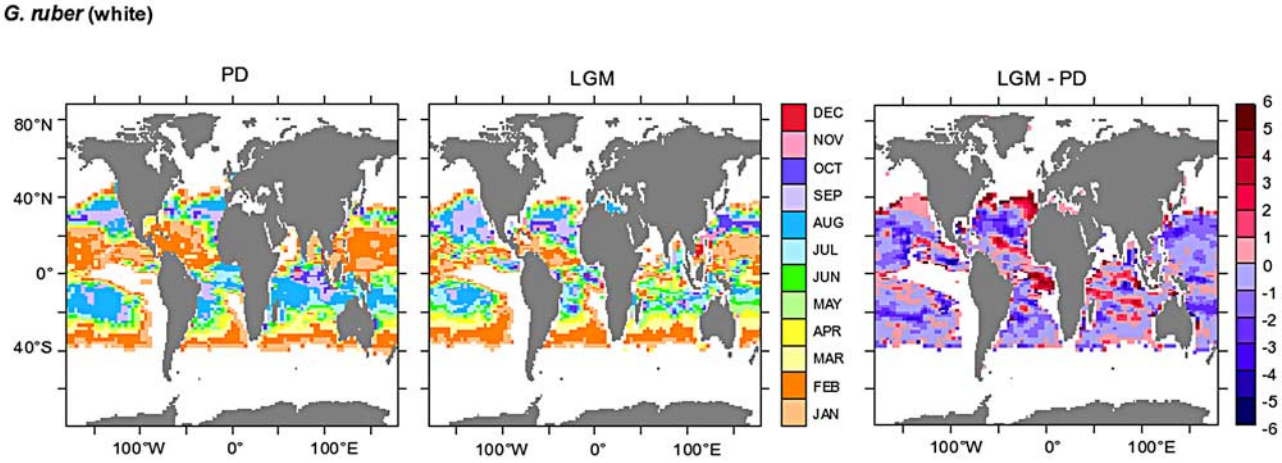

Figure 12. Maximum production month of *G. ruber* (white) at PD, LGM, and the difference between both (in months). Positive values indicate that during the LGM the maximum production was later in the year.

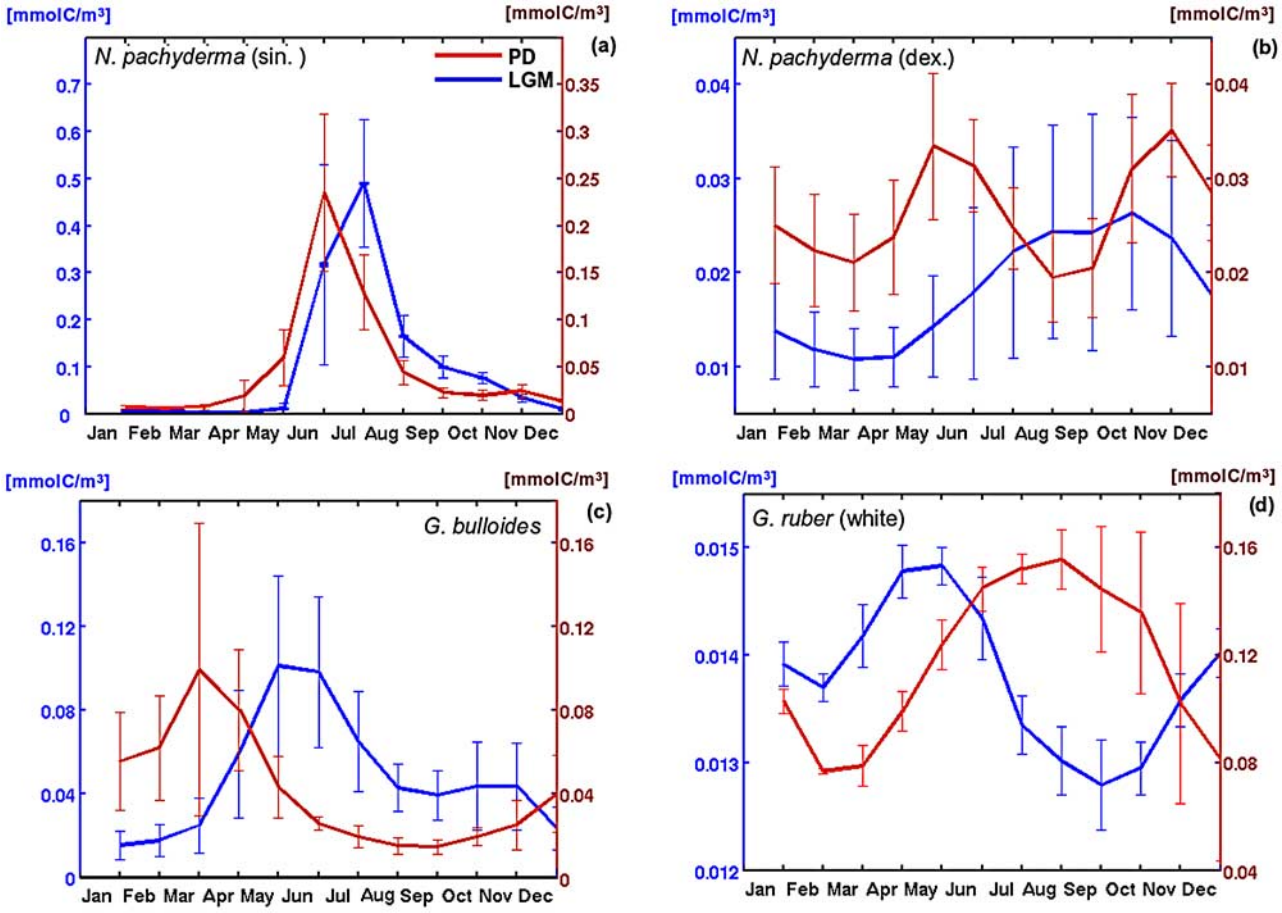

Figure 13. Examples of modeled annual biomass (mmolC/m^3) variation of (a) *N. pachyderma* (sinistral) in the North Atlantic (52°–56°N, 36°–43°W), (b) *N. pachyderma* (dextral) in the North Pacific (36°–39°N, 151°–158°E), (c) *G. bulloides* in the North Atlantic (39°–43°N, 47°–54°W), and (d) *G. ruber* (white) in the South Atlantic (22°–25°S, 22°–30°W) at PD (red) and LGM (blue). Lines represent mean values, and error bars represent standard deviations over the region.

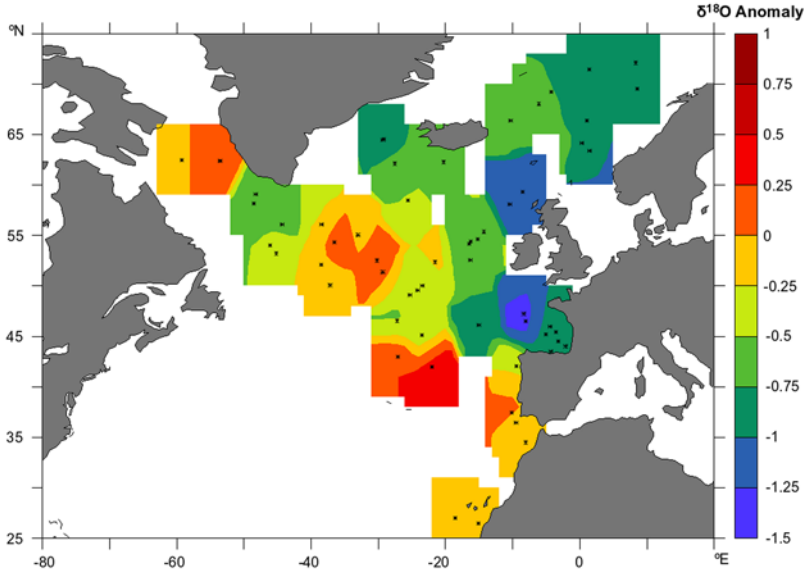

Figure 14. Reconstructed seawater δ^{18}O anomaly in the northern North Atlantic at the LGM (LGM – modern – 1.2) using planktonic foraminifera. Data from *Duplessy et al.* [1991].

the maximum production of subtropical and high-latitude foraminifera generally occurred at a warmer season of the year. Some of these results may not be new in concept, but they are here derived for the first time from a comprehensive modeling approach.

[34] Changes in seasonality of the species recording a seasonal proxy signal, in particular species living at high latitudes associated with high temperature seasonality, have implications for paleoceanographic reconstructions. In contrast, for the species living in tropical waters the change in seasonality did not produce an important bias in estimated temperature, as the amplitude of the annual cycle of SST is relatively low, and therefore the recorded temperature is close to the annual mean SST.

[35] The increase of nutrients globally by 3.2% has little effect in the abundance of foraminifera. In contrast, The redistribution of nutrients below mixed layer, according to UVic simulated glacial conditions, alters the biomass of foraminifera in the mixed layer. However, these variations of the biomass do not influence substantially the recorded temperature signal by a species.

[36] **Acknowledgments.** We would like to thank J. Ortiz and an anonymous reviewer for their careful review, their constructive critique,

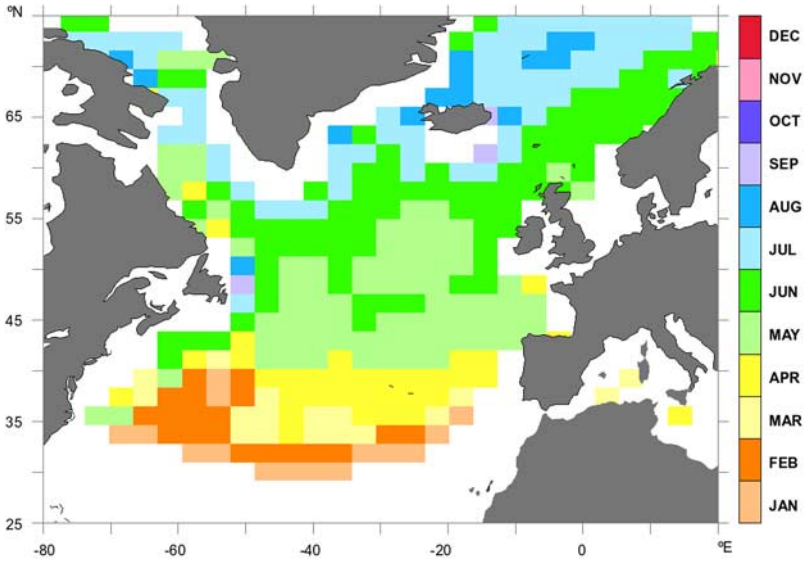

Figure 15. Maximum production month of *N. pachyderma* (sinistral) during the Last Glacial Maximum in the northern North Atlantic.

the hints to a number of critical points, and their useful suggestions to improve the manuscript. The CCSM3 climate model runs were performed on the IBM pSeries 690 supercomputer of the Norddeutscher Verbund für Hoch- und Höchstleistungsrechnen. This project was supported by the DFG as part of the European Graduate College Proxies in Earth History and the DFG Research Center/Excellence Cluster, the Ocean in the Earth System.

References

Arnold, A. J., and W. C. Parker (1999), Biogeography of planktonic foraminifera, in *Modern Foraminifera*, edited by B. K. S. Gupta, pp. 103–122, Kluwer Acad., Dordrecht, Netherlands.

Barrows, T., and S. Juggins (2004), Compilation of planktic foraminifera LGM assembages from the Indo-Pacific Ocean, http://doi.pangaea.de/10.1594/PANGAEA.227319, doi:10.1594/PANGAEA.227319, PANGAEA, Network for Geol. and Environ. Data, Bremerhaven, Germany.

Bé, A. W. H. (1960), Ecology of recent planktonic foraminifera: Part 2—Bathymetric and seasonal distributions in the Sargasso Sea off Bermuda, *Micropaleontology*, *6*, 373–392.

Bé, A. W. H. (1982), Biology of planktonic foraminifera, in *Foraminifera: Notes for a Short Course*, edited by T. W. Broadhead, pp. 51–92, Univ. of Tenn., Knoxville.

Bé, A. W. H., and W. H. Hamilton (1967), Ecology of recent planktonic foraminifera, *Micropaleontology*, *13*, 87–106.

Bé, A. W. H., and D. S. Tolderlund (1971), Distribution and ecology of living planktonic foraminifera in surface waters of the Atlantic and Indian oceans, in *The Micropalaeontology of Oceans*, edited by B. M. Funnell and W. R. Riedel, pp. 105–149, Cambridge Univ. Press, U. K.

Bijma, J., W. W. J. Faber, and C. Hemleben (1990), Temperature and salinity limits for growth and survival of some planktonic foraminifers in laboratory cultures, *J. Foraminiferal Res.*, *20*, 95–116.

Bishop, J. K. B., and W. B. Rossow (1991), Spatial and temporal variability of global surface solar irradiance, *J. Geophys. Res.*, *96*, 16,839–16,858.

Braconnot, P., et al. (2007), Results of PMIP2 coupled simulations of the Mid-Holocene and Last Glacial Maximum—Part 1: Experiments and large-scale features, *Clim. Past*, *3*, 261–277.

Cavalieri, D., P. Gloerson, and J. Zwally (1990), DMSP SSM/I daily polar gridded sea ice concentrations, October 1998 to September 1999, http://nsidc.org/data/nsidc-0081.html, for Natl. Snow and Ice Data Cent., Boulder, Colo.

Collins, W. D., M. L. Blackmon, G. B. Bonan, J. J. Hack, T. B. Henderson, J. T. Kiehl, W. G. Large, and D. S. McKenna (2006), The Community Climate System Model version 3 (CCSM3), *J. Clim.*, *19*, 2122–2143.

Conkright, M., S. Levitus, T. O'Brien, T. Boyer, J. Antonov, and C. Stephens (1998), World Ocean Atlas 1998 CD-ROM data set documentation, *Tech. Rep. 15*, Natl. Oceanogr. Data Cent., Silver Spring, Md.

Cox, P. M. (2001), Description of the "TRIFFID" dynamic global vegetation model, *Tech. Note 24*, Hadley Cent., Bracknell, U. K.

Cox, P. M., R. A. Betts, C. B. Bunton, R. L. H. Essery, P. R. Rowntree, and J. Smith (1999), The impact of new land surface physics on the GCM simulation of climate and climate sensitivity, *Clim. Dyn.*, *15*, 183–203.

Deuser, W. G., E. H. Ross, C. Hemleben, and M. Spindler (1981), Seasonal changes in species composition, numbers, mass, size, and isotopic composition of planktonic foraminifera settling into the deep Sargasso Sea, *Palaeogeogr. Palaeoclimatol. Palaeoecol.*, *33*, 103–127.

Duplessy, J. C., L. Labeyrie, A. Juillet-Leclerc, F. Maitre, J. Duprat, and M. Sarnthein (1991), Surface salinity reconstruction of the North Atlantic Ocean during the Last Glacial Maximum, *Oceanol. Acta*, *14*, 311–324.

Fairbanks, R. G. (1989), A 17,000-year glacio-eustatic sea level record: Influence of glacial melting rates on the Younger Dryas event and deep-ocean circulation, *Nature*, *342*, 637–642.

Fraile, I., M. Schulz, S. Mulitza, and M. Kucera (2008), Predicting the global distribution of planktonic foraminifera using a dynamic ecosystem model, *Biogeosciences*, *5*, 891–911.

Fraile, I., S. Mulitza, and M. Schulz (2009), Modeling planktonic foraminiferal seasonality: Implications for temperature reconstructions, *Mar. Micropaleontol.*, doi:10.1016/j.marmicro.2009.01.003, in press.

Gent, P. R., F. O. Bryan, G. Danabasoglu, S. C. Doney, W. R. Holland, W. G. Large, and J. C. McWilliams (1998), The NCAR climate system model global ocean component, *J. Clim.*, *11*, 1287–1306.

Hemleben, C., M. Spindler, and O. R. Anderson (1989), *Modern Planktonic Foraminifera*, Springer, New York.

Honjo, S., and K. W. Doherty (1988), Large aperture time-series sediment traps: Design objectives, construction and application, *Deep Sea Res., Part A*, *35*, 133–149.

Honjo, S., J. F. Connell, and P. L. Sachs (1980), Deep-ocean sediment trap: Design and function of PARFLUX Mark II, *Deep Sea Res., Part A*, *27*, 745–753.

Kalnay, E., et al. (1996), The NCEP/NCAR 40-year reanalysis project, *Bull. Am. Meteorol. Soc.*, *77*, 437–471.

King, A. L., and W. R. Howard (2005), $\delta^{18}O$ seasonality of planktonic foraminifera from Southern Ocean sediment traps: Latitudinal gradients and implications for paleoclimate reconstructions, *Mar. Micropaleontol.*, *56*, 1–24.

Kucera, M., et al. (2004a), Compilation of planktic foraminifera census data, LGM from the Pacific Ocean, http://doi.pangaea.de/10.1594/PANGAEA.227329, doi:10.1594/PANGAEA.227329, PANGAEA, Network for Geol. and Environ. Data, Bremerhaven, Germany.

Kucera, M., et al. (2004b), Compilation of planktic foraminifera census data, LGM and SSTs from the Pacific Ocean, http://doi.pangaea.de/10.1594/PANGAEA.227325, doi:10.1594/PANGAEA.227325, PANGAEA, Network for Geol. and Environ. Data, Bremerhaven, Germany.

Kucera, M., A. Rosell-Melé, R. Schneider, C. Waelbroeck, and M. Weinelt (2005a), Multiproxy approach for the reconstruction of the glacial ocean surface (MARGO), *Quat. Sci. Rev.*, *24*, 813–819.

Kucera, M., et al. (2005b), Reconstruction of sea-surface temperatures from assemblages of planktonic foraminifera: Multi-technique approach based on geographically constrained calibration data sets and its application to glacial Atlantic and Pacific oceans, *Quat. Sci. Rev.*, *24*, 951–998.

Labeyrie, L. D., J. C. Duplessy, J. Duprat, A. Juillet-Leclerc, J. Moyes, E. Michel, N. Kallel, and N. J. Shackleton (1992), Changes in vertical structure of the North Atlantic Ocean between glacial and modern times, *Quat. Sci. Rev.*, *11*, 401–413.

Lombard, F., L. Labeyrie, E. Michel, H. J. Spero, and D. Lea (2009), Modelling the temperature dependent growth rates of planktic foraminifera, *Mar. Micropaleontol.*, *70*, 1–7.

Mahowald, N., K. Kohfeld, M. Hansson, Y. Balkanski, S. P. Harrison, I. C. Prentice, M. Schulz, and H. Rodhe (1999), Dust sources and deposition during the Last Glacial Maximum and current climate: A comparison of model results with paleodata from ice cores and marine sediments, *J. Geophys. Res.*, *104*, 15,895–15,916.

Martinez, J. I., L. Taylor, P. Deckker, and T. Barrows (1998), Planktonic foraminifera from the eastern Indian Ocean: Distribution and ecology in relation to the Western Pacific Warm Pool (WPWP), *Mar. Micropaleontol.*, *34*, 121–151.

Meissner, K. J., A. J. Weaver, H. D. Matthews, and P. M. Cox (2003), The role of land surface dynamics in glacial inception: A study with the UVic Earth System Model, *Clim. Dyn.*, *21*, 515–527, doi:10.1007/s00382-003-0352-2.

Mix, A. (1987), The oxygen-isotope record of glaciation, in *The Geology of North America*, vol. K-3, *North America and Adjacent Oceans During the Last Deglaciation*, edited by W. F. Ruddiman and H. E. Wright Jr., pp. 111–135, Geol. Soc. of Am., Boulder, Colo.

Monterey, G., and S. Levitus (1997), *Seasonal Variability of Mixed Layer Depth for the World Ocean, NOAA Atlas NESDIS*, vol. 14, NOAA, Silver Spring, Md.

Moore, J. K., S. C. Doney, J. A. Kleypas, D. M. Glover, and I. Y. Fung (2002), An intermediate complexity marine ecosystem model for the global domain, *Deep Sea Res., Part II*, *49*, 403–462.

Mulitza, S., T. Wolff, J. Pätzold, W. Hale, and G. Wefer (1998), Temperature sensitivity of planktic foraminifera and its influence on the oxygen isotope record, *Mar. Micropaleontol.*, *33*, 223–240.

Niebler, H.-S. (2004), Assemblage of planktonic foraminifera for the Last Glacial Maximum (LGM) in sediment cores from the South Atlantic, http://doi.pangaea.de/10.1594/PANGAEA.55260, doi:10.1594/PANGAEA.55260, PANGAEA, Network for Geol. and Environ. Data, Bremerhaven, Germany.

Otto-Bliesner, B. L., E. C. Brady, G. Clauzet, R. Tomas, S. Levis, and Z. Kothavala (2006a), Last Glacial Maximum and Holocene climate in CCSM3, *J. Clim.*, *19*, 2526–2544.

Otto-Bliesner, B. L., R. Tomas, E. C. Brady, C. Ammann, Z. Kothavala, and G. Clauzet (2006b), Climate sensitivity of moderate- and low-resolution versions of CCSM3 to preindustrial forcings, *J. Clim.*, *19*, 2567–2583.

Peltier, W. R. (2004), Global glacial isostasy and the surface of the ice-age Earth: The ICE-5G (VM2) model and GRACE, *Annu. Rev. Earth Planet. Sci.*, *32*, 111–149.

Pflaumann, U., J. Duprat, C. Pujol, and L. D. Labeyrie (1996), SIMMAX: A modern analog technique to deduce Atlantic sea surface temperatures from planktonic foraminifera in deep-sea sediments, *Paleoceanography*, *11*, 15–35.

Pflaumann, U., et al. (2003), Glacial North Atlantic: Sea-surface conditions reconstructed by GLAMAP 2000, *Paleoceanography*, *18*(3), 1065, doi:10.1029/2002PA000774.

Prange, M. (2008), The low-resolution CCSM2 revisited: New adjustments and a present-day control run, *Ocean Sci.*, *4*, 151–181.

Prell, W. L., A. Martin, J. Cullen, and M. Trend (1999), Brown University Foraminiferal Database, IGBP PAGES/WDCA Data Contrib. Ser. 1999-027, http://www.ncdc.noaa.gov/paleo/metadata/noaa-ocean-5908.html, for World Data Cent. Paleoclimatology, Natl. Geophys. Data Cent., NOAA, Boulder, Colo.

Rossow, W. B., and R. A. Schiffer (1991), ISCCP cloud data products, *Bull. Am. Meteorol. Soc.*, *72*, 2–20.

Sarnthein, M., K. Winn, S. J. A. Jung, J.-C. Duplessy, L. Labeyrie, H. Erlenkeuser, and G. Ganssen (1994), Changes in East Atlantic deepwater circulation over the last 30000 years: Eight time slice reconstructions, *Paleoceanography*, *9*, 209–267.

Sarnthein, M., et al. (1995), Variations in Atlantic surface ocean paleoceanography, 50°–80°N: A time-slice record of the last 30,000 years, *Paleoceanography*, *10*, 1063–1094.

Sautter, L. R., and R. C. Thunell (1991), Planktonic foraminiferal response to upwelling and seasonal hydrographic conditions: Sediment trap results from San Pedro Basin, *Southern California Bight, J. Foraminiferal Res.*, *21*, 347–363.

Schäfer-Neth, C., and A. Paul (2001), Circulation of the glacial Atlantic: A synthesis of global and regional modeling, in *The Northern North Atlantic: A Changing Environment*, edited by P. Schäfer et al., pp. 441–462, Springer, Berlin.

Schiebel, R., and D. Hemleben (2005), Modern planktic foraminifera, *Palaeontol. Z.*, *79*, 135–148.

Schmittner, A., A. Oschlies, X. Giraud, M. Eby, and H. L. Simmons (2005), A global model of the marine ecosystem for long-term simulations: Sensitivity to ocean mixing, buoyancy forcing, particle sinking, and dissolved organic matter cycling, *Global Biogeochem. Cycles*, *19*, GB3004, doi:10.1029/2004GB002283.

Tedesco, K., R. Thunell, Y. Astor, and F. Muller-Karger (2007), The oxygen isotope composition of planktonic foraminifera from the Cariaco basin, Venezuela: Seasonal and interannual variations, *Mar. Micropaleontol.*, *62*, 180–193.

Thunell, R. C., and S. Honjo (1987), Seasonal and interannual changes in the planktonic foraminiferal production in the North Pacific, *Nature*, *328*, 335–337.

Waelbroeck, C., et al. (2009), Constraints on the magnitude and patterns of ocean cooling at the Last Glacial Maximum, *Nat. Geosci.*, *2*, 127–132, doi:10.1038/ngeo411.

Watkins, J. M., and A. C. Mix (1998), Testing the effects of tropical temperature, productivity, and mixed-layer depth on foraminiferal transfer functions, *Paleoceanography*, *13*, 96–105.

Watkins, J. M., A. C. Mix, and J. Wilson (1996), Living planktic foraminifera: Tracers of circulation and productivity regimes in the central equatorial Pacific, *Deep Sea Res., Part II*, *43*, 1257–1282.

Weaver, A. J., et al. (2001), The UVic Earth System Climate Model: Model description, climatology, and applications to past, present and future climates, *Atmos. Ocean*, *39*, 361–428.

Weinelt, M., M. Sarnthein, U. Pflaumann, H. Schulz, S. J. A. Jung, and H. Erlenkeuser (1996), Ice-free Nordic Seas during the Last Glacial Maximum? Potential sites of deepwater formation, *Paleoclimates*, *1*, 283–309.

Weinelt, M., MARGO, and SST (2004), Compilation of global planktic foraminifera LGM SST data, http://doi.pangaea.de/10.1594/PANGAEA.227620, doi:10.1594/PANGAEA.227620, PANGAEA, Network for Geol. and Environ. Data, Bremerhaven, Germany.

Yeager, S. G, C. A. Shields, W. G. Large, and J. J. Hack (2006), The low-resolution CCSM3, *J. Clim.*, *19*, 2545–2566.

Žarić, S., B. Donner, G. Fischer, S. Mulitza, and G. Wefer (2005), Sensitivity of planktic foraminifera to sea surface temperature and export production as derived from sediment trap data, *Mar. Micropaleontol.*, *55*, 75–105.

I. Fraile, Faculty of Geosciences, University of Bremen, D-28334 Bremen, Germany. (iugalde@marum.de)

U. Merkel, S. Mulitza, A. Paul, M. Prange, and M. Schulz, MARUM, University of Bremen, D-28334 Bremen, Germany.